August 27-31, 2023
FLORENCE - ITALY
ICWE 16
16th International Conference on Wind Engineering

Role of spanwise correlation in the vortex-induced vibration of a non-streamlined bridge deck section

Bernardo Nicese [1], Cong Chen [2], Antonino Maria Marra [3], Gianni Bartoli [1], Klaus Thiele [2], Claudio Mannini [1]

[1]*CRIACIV/Dept. of Civil and Environmental Engineering, Univ. of Florence, Via S. Marta 3, Florence, Italy, bernardo.nicese@unifi.it, gianni.bartoli@unifi.it, claudio.mannini@unifi.it*
[2]*Inst. of Steel Structures, Technische Universität Braunschweig, Beethovenstr. 51, Brunswick, Germany, c.chen@stahlbau.tu-braunschweig.de, k.thiele@stahlbau.tu-braunschweig.de*
[3]*CRIACIV/Dept. of Architecture, Univ. of Florence, Piazza Brunelleschi 6, Florence, Italy, antoninomaria.marra@unifi.it*

SUMMARY: The present work aims to investigate the spanwise correlation of the vortex-shedding fluctuating force acting on a bridge deck sectional model. To this purpose, a realistic bridge section characterized by a non-streamlined geometry is chosen. The model is tested with and without lateral traffic barriers for different wind angles of attack. Force and pressure measurements are carried out on the stationary model, and lateral barriers are found to produce an increase of the spanwise pressure correlation. This conclusion can be inferred by the comparison between the global lateral force measured on the sectional model and the sectional force obtained by pressure integration. This result is also confirmed by the analysis of the decay of pressure correlation along some specific spanwise arrays of taps. Then, aeroelastic tests are carried out when the model is free to vibrate, and pressures are measured along a few spanwise arrays of taps in lock-in condition. The body motion leads to an almost full spanwise correlation of pressures along the arrays considered, both with and without barriers, even for a small vibration amplitude.

Keywords: vortex-induced vibration, bridge decks, spanwise correlation

1. INTRODUCTION

Vortex-induced vibration (VIV) is a phenomenon frequently observed for bridge decks, especially in the case of low damping combined with a limited mass per unit length. VIV can represent a problem for a bridge mainly due to the discomfort for users and possible fatigue damage too. VIV affects not only slender decks typical of suspension or cable-stayed bridges, but also girder bridges characterized by a limited span length and a non-streamlined cross section. It is known that VIV leads to an increase in the spanwise correlation of the fluctuating forces, depending on the vibration amplitude and the excited modal shape of the structure. The growth of fluctuating force correlation at lock-in is also at the base of some mathematical models for VIV (*e.g.*, Ruscheweyh, 1990). In particular, a correlation increase of the vortex-shedding pressure fluctuations implies a growth of the lateral force acting on the vibrating body, which is a key parameter for a variety of wake-oscillator models to predict the VIV response (*e.g.*, Chen et al., 2022). Investigations of spanwise correlation of pressures and forces measured on vibrating cylinders usually concern simplified and paradigmatic geometries like circular, square and rectangular cylinders (*e.g.*, Wilkinson, 1981;

Ricciardelli, 2010, Marra et al., 2017), while only few studies refer to bridge deck sections (*e.g.*, Sun et al., 2019). This work focuses on the spanwise correlation of the VIV forces acting on a wind tunnel bridge sectional model, characterized by a non-streamlined geometry. Both the stationary state and the lock-in regime are considered in terms of pressure and force correlation and in terms of lateral force fluctuation amplitude.

2. WIND TUNNEL TESTS

2.1 Wind tunnel facility, setups and model

The tests are carried out in the boundary layer wind tunnel at the Institute of Steel Structures of the Technische Universität Braunschweig, Germany. The wind tunnel is a suction Eiffel-type facility with a rectangular cross section 1.4 m wide and 1.2 m high. The flow velocity can continuously be varied up to about 25 m/s. The sectional model (Fig. 1) is inspired by the Great Belt East Bridge approaching spans (Schewe and Larsen, 1998). The model is 6 cm deep (D), 22.1 cm wide (B), has a lower side width of 9.4 cm (b), and is 1.2 m long (L). The side ratio B/D is about 3.7, while the aspect ratio L/D is equal to 20. The model is made of a top and a bottom aluminum plate, longitudinally connected by two 3D-printed corner elements (the colored filled parts in Fig. 1(a). The model is internally stiffened by a square aluminum tube with a side of 4 cm and 12 plastic ribs. The model can be opened at any time by removing the upper plate and is equipped with holes for installing pressure tubes. Several cross sections are equipped with 32 pressure taps distributed along the perimeter. Moreover, longitudinal arrays of taps are available at different distances from the leading edge on the upper and lower sides, for the evaluation of pressure spanwise correlation. The model is equipped with two lateral traffic barriers (Fig. 1(c)), whose geometry aims to reproduce as well as possible the real barriers installed on the bridge prototype (Fig. 1(d)).

Static force measurements are performed by means of load cells, over a broad range of flow angles of attack (α). Pressure measurements are carried out in the midspan section of the stationary model and along longitudinal arrays for null, 3° and -3° angles of attack. Then, the model is also elastically suspended by means of eight coil springs and let free to vibrate for the same three angles

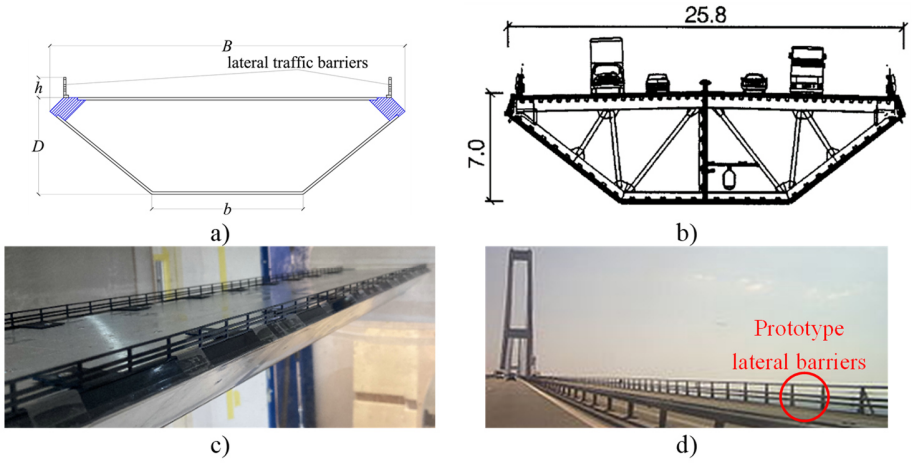

Figure 1. Cross section of the model (a) and cross section of the prototype with dimensions indicated in m (b) (Schewe and Larsen, 1998). Close up of the scale (c) and real (d) lateral traffic barriers.

of attack to determine the VIV response. The transverse displacement of the model is measured, along with the pressures along a tap array located on the top side at 0.86B from the leading edge, to investigate the change in the vortex-shedding force correlation due to the body motion. Tests are carried out for both the bare deck and the deck equipped with lateral barriers.

2.2 Test results

Static tests are carried out to determine the aerodynamic behavior of the bridge section in terms of forces and pressures, over a broad range of angles of attack. The Strouhal number (St) is also estimated, with a value for the bare deck at $\alpha = 0°$ very close to that found by Schewe and Larsen (1998), although for a higher Reynolds number (St = 0.22). The lift coefficient power spectral density is integrated around the Strouhal frequency to estimate the amplitude of the dimensionless vortex-shedding lateral force (C_{L0}). When this coefficient is estimated by pressure integration over the midspan cross section is denoted as $C_{L0,p}$, while when it is determined by force measurements it is denoted as $C_{L0,f}$ (Table 1). The former represents the sectional lift fluctuation, while the latter is an average over the deck model. The larger is the difference between them, the shorter is the spanwise correlation length of the vortex-shedding force compared to L. The results show that the lateral barriers remarkably increase the spanwise correlation of the vortex-shedding force.

Aeroelastic test results (Fig. 2) emphasize the effect of the lateral barriers, which lead to a larger transverse vibration (y) and a wider lock-in range in terms of reduced velocity $U = V/n_0D$, where V is the wind speed and n_0 is the natural frequency of the system. Pressures along the abovementioned longitudinal tap array are also measured during aeroelastic tests for the vibrating model. Fig. 3 reports the pressure spanwise correlation coefficient (R_p) for the stationary body and for the peak vibration amplitude observed at lock-in, in case of both bare deck (y_0) and deck

Table 1. Values of the Strouhal number (St) and lateral coefficient fluctuation amplitude determined through force ($C_{L0,f}$) and pressure ($C_{L0,p}$) measurements, for the configurations with and without barriers for different angles of attack. All coefficients are normalized with the bare deck depth D.

	Layout	St	$C_{L0,f}$	$C_{L0,p}$	$C_{L0,f}/C_{L0,p}$
$\alpha = 0°$	Bare deck	0.217	0.06	0.12	0.50
	Barrier	0.155	0.34	0.38	0.89
$\alpha = 3°$	Bare deck	0.197	0.07	0.15	0.47
	Barrier	0.148	0.40	0.42	0.95
$\alpha = -3°$	Bare deck	0.177	0.24	0.42	0.57
	Barrier	0.154	0.39	0.56	0.70

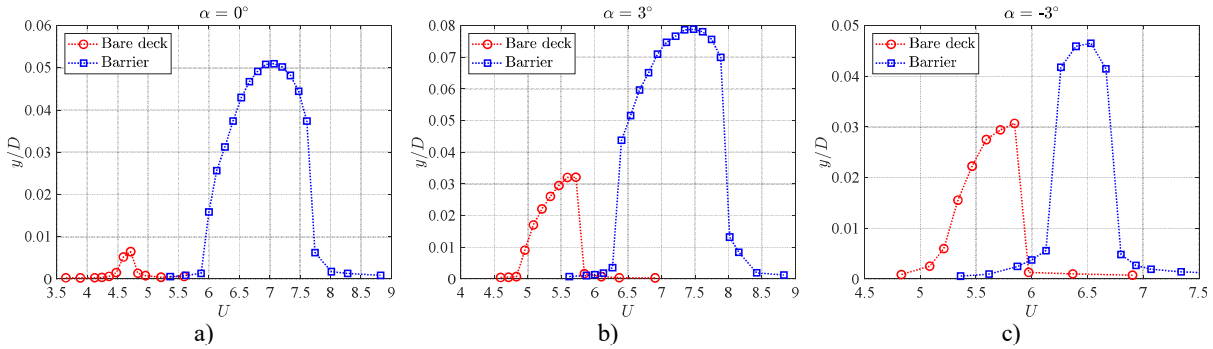

Figure 2. Response curve at lock-in for the deck model with and without traffic barriers at null (a), 3° (b) and -3° (c) wind angle of attack, in terms of dimensionless transverse vibration amplitude y/D against flow reduced velocity U.

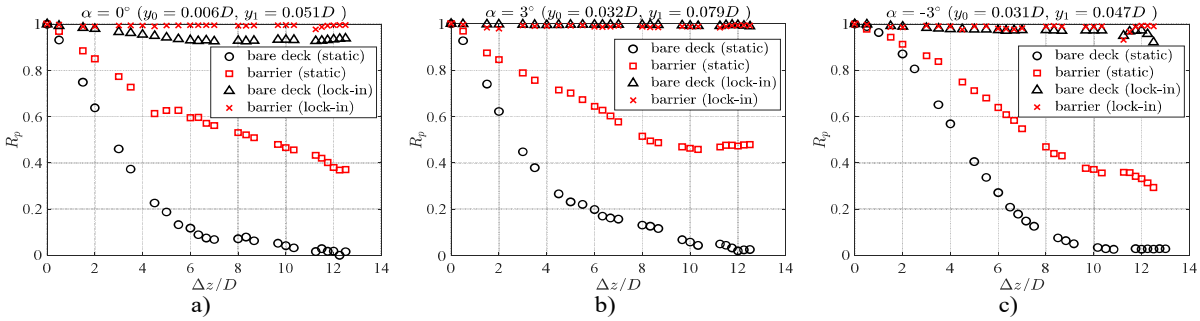

Figure 3. Spanwise pressure correlation coefficient (R_p) along a top longitudinal tap array, at $0.86B$ from the leading edge, with and without lateral barriers for angles of attack 0°, -3° and 3°, for the stationary and the vibrating model (peak vibration at lock-in). The longitudinal distance between two positions (Δz) is normalized with D.

equipped with lateral barriers (y_1). The results for the stationary case remark what suggested by the lateral coefficient values (Table 1): the decay of pressure correlation is much faster for the bare deck compared to the layout with barriers for all the angles of attack tested. For the vibrating model, interestingly, an almost perfect correlation along the tap array is measured even for a small oscillation amplitude (lower than $0.01D$ for the bare deck at a null angle of attack), independently of the correlation experienced in the stationary condition.

3 PROSPECTS

The next work phase, which will be dealt with in the full paper, aims to extend pressure measurements on the vibrating model to a few cross sections simultaneously, since pressures along a specific spanwise array cannot fully describe the correlation of the vortex-shedding force acting on the sectional model. In addition, pressure measurements around the deck cross-section in dynamic conditions allow estimating the magnitude of the fluctuating sectional force, which can be compared to that measured on the stationary model. Finally, aeroelastic tests will be repeated for different values of the mass-damping parameter of the system, so that pressures and forces can be evaluated for different vibration amplitudes at the same reduced frequency.

REFERENCES

Chen, C., Mannini, C., Bartoli, G., and Thiele, K., 2022. Wake oscillator modeling the combined instability of vortex induced vibration and galloping for a 2:1 rectangular cylinder. Journal of Fluids and Structures 110, 103530.

Marra, A. M., Mannini, C., and Bartoli G., 2017. Wind tunnel modeling for the vortex-induced vibrations of a yawed bridge tower. Journal of Bridge Engineering 22 (5), 04017006.

Ricciardelli, 2010. Effects of the vibration regime on the spanwise correlation of the aerodynamic forces on a 5:1 rectangular cylinder. Journal of Wind Engineering and Industrial Aerodynamics 98, 215-225.

Ruscheweyh, H., 1990. Practical experiences with wind-induced vibrations. Journal of Wind Engineering and Industrial Aerodynamics 33, 211–218.

Schewe, G. and Larsen, A., 1998. Reynolds number effects in the flow around a bluff bridge deck cross section. Journal of Wind Engineering and Industrial Aerodynamics 74-76, 829–838.

Sun, Y., Li, M., Li, M., and Liao, H., 1998. Spanwise correlation of vortex-induced forces on typical bluff bodies. Journal of Wind Engineering and Industrial Aerodynamics 189, 186–197.

Wilkinson, R. H., 1981. Fluctuating pressures on an oscillating square prism. Part II. Spanwise correlation and loading. The Aeronautical Quarterly 32 (2), 111–125.